MIXED CONVECTION IN A SQUARE CAVITY WITH A HEAT-CONDUCTING HORIZONTAL SQUARE CYLINDER

Md. Mustafizur Rahman[1*], M. A. Alim[1] and Sumon Saha[2]

Received: Jun 18, 2009; Revised: Oct 6, 2009; Accepted: Oct 15, 2009

Abstract

The problem of mixed convection heat transfer in a square cavity with a centered heat conducting horizontal square solid cylinder is analyzed in this paper. As boundary conditions of the cavity, the right vertical wall is kept at constant temperature and the remaining three walls are kept thermally insulated. An external flow enters the cavity through an opening in the left vertical wall and exits from another opening in the right vertical wall. This configuration leads to a conjugate heat transfer problem and simulates the cooling of electronic equipments. Emphasis is placed on the influences of the governing parameters, such as Reynolds number, Richardson number, Prandtl number and the inlet and exit port locations of the cavity. The coupled equations of the simulated model are solved numerically using finite element method. Finally, parametric results are presented in terms of streamlines, isotherms, average Nusselt number at the heated wall, average temperature of the fluid and the temperature at the cylinder center in the cavity. The computational results indicate that Reynolds number has significant effect on the flow field in the pure forced convection and in the pure mixed convection region, but Prandtl number has significant effect on the flow field in the pure mixed convection and in the free convection dominated region. On the other hand, the mentioned parameters have significant effect on the thermal field in the three convective regimes considered. Lastly, the locations of the inlet and outlet port have significant effect on both the flow and thermal fields in the three convective regimes.

Keywords: Heat transfer, finite element method, mixed convection, square cylinder, square cavity

Introduction

Mixed convection flows are present in many transport processes in nature and in engineering devices. Examples of mixed convection flows can be found in heat exchangers, nuclear reactors, solar energy storage, heat rejection systems, heaters and refrigeration devices, etc (Papanicolaou and Jaluria, 1990). Analysis of above phenomena incorporating a solid heat conducting obstruction extends its usability to various other practical situations (Papanicolaou and Jaluria, 1993). Particularly, a conductive material in an inert atmosphere inside a furnace with a constant

[1] *Department of Mathematics, Bangladesh University of Engineering & Technology (BUET), Dhaka-1000, Bangladesh. E-mail: mmustafizurrahman@math.ac.bd, s.saha2@pgrad.unimelb.edu.au*

[2] *Department of Mechanical Engineering, University of Melbourne, Victoria 3010, Australia.*

[*] *Corresponding author*

flow of gas from outside constitutes apractical application for the present study. Many authors have recently studied heat transfer in enclosures with partitions, thereby altering the convection flow phenomenon.

Hsu and Wang (2000) numerically studied the mixed convective heat transfer where the heat source was embedded on a board mounted vertically on the bottom wall at the middle in the enclosure. The cooling airflow enters and exits the enclosure through the openings near the top of the vertical sidewalls. They showed that both the thermal and flow field depend strongly on the governing parameters, the position of the heat source as well as the property of the heat source- embedded-board. Angirasa (2000) conducted a numerical study to investigate the complex interaction between buoyancy and forced flow in a square enclosure with an inlet and a vent situated respectively, at the bottom and top edges of the vertical isothermal surface, where the other three walls are adiabatic. She concluded that for the aiding buoyancies, the through flow induces a clockwise eddy whose strength depends on the Reynolds number and heat transfer is augmented with increasing Reynolds number. However, at the higher range of Reynolds numbers, the local heat transfer characteristics change. Omri and Nasrallah (1999) considered mixed convection in an air-cooled cavity with differentially heated vertical isothermal sidewalls having inlet and exit ports by a control volume finite element method. They investigated two different placement configurations of the inlet and exit ports on the sidewalls. Best configuration was selected to analyze the cooling effectiveness of the cavity, which suggested that injecting air through the cold wall was more effective in heat removal and placing inlet near the bottom and exit near the top produced effective cooling. Later on, Singh and Sharif (2003) extended their works by considering six placement configurations of the inlet and outlet of a differentially heated rectangular enclosure whereas the previous work was limited to only two different configurations of inlet and outlet. At the same time, Manca *et al*. (2003) presented a numerical analysis of laminar mixed convection in an open cavity with a heated wall bounded by a horizontally insulated plate, where they were considered three heating modes: assisting flow, opposing flow, and heating from below, and the results were reported for Richardson number from 0.1 to 100, Reynolds numbers from 100 to 1000, and aspect ratio in the range 0.1-1.5. It was shown that the maximum temperature values decrease as the Reynolds and the Richardson numbers increase. The effect of the ratio of channel height to the cavity height wasfound to play a significant role on streamline and isotherm patterns for different heating configurations. The investigation also indicated that opposing forced flow configuration has the highest thermal performance, in terms of both maximum temperature and average Nusselt number. Later on, Manca *et al*. (2006) tested experimentally the similar problem for the case of assisting forced flow configuration. Based on the flow visualization results, they pointed out that for Re = 1000, there were two nearly distinct fluid motions: a parallel forced flow in the channel and a recirculation flow inside the cavity. Lastly for Re = 100 the effect of a stronger buoyancy determined a penetration of thermal plume from the heated plate wall into the upper channel.

Convection in enclosures containing blocks has gained recent research significance as a means of heat transfer enhancement. One of the systematic numerical investigations of this problem was conducted by House *et al*. (1990), who considered natural convection in a vertical square cavity with heat conducting body, placed on center in order to understand the effect of the heat conducting body on the heat transfer process in the cavity. They found that the heat transfer across the enclosures enhanced by a body with thermal conductivity ratio less than unity. Lacroix and Joyeux (1995) conducted a numerical study of natural convection heat transfer from two horizontal heated cylinders confined to a rectangular enclosure having finite wall conductance. They indicated that wall heat conduction reduces the average temperature differences across the cavity, partially stabilizes the flow and decreases natural convection heat transfer around the

cylinders. Braga and Lemos (2005) numerically studied steady laminar natural convection within a square cavity filled with a fixed amount of conducting solid material consisting of either circular or square obstacles. They showed that the average Nusselt number for cylindrical rods is slightly lower than those for square rods. Lee and Ha (2005) investigated natural convection in a horizontal layer of fluid with a conducting body in the interior, using an accurate and efficient Chebyshev spectral collocation approach. Very recently, Rahman *et al.* (2009) studied mixed convection in a rectangular cavity with a heat-conducting horizontal circular cylinder by finite element method.

Motivated by previous works, the objective of the present study is to examine the influence of the Reynolds numbers, Prandtl numbers and four inlet and outlet locations of the cavity at the three values of Richardson numbers on the characteristics of combined free and forced convection flow inside a square cavity containing a solid heat conducting horizontal square cylinder of diameter D = 0.2 and solid fluid thermal conductivity ratio K = 5.0. A finite element approach is employed to solve the two dimensional Navier-stokes equations along with energy equations for laminar flow of an incompressible fluid. The phenomena of fluid flow and temperature distributions inside the cavity are explained in detail.

Model Specification

Figure 1 shows a schematic diagram of the system and the coordinates. Only a square enclosure is considered. The problem is considered to be two-dimensional. The right vertical wall is maintained at a temperature (T_h), whereas the other walls (i.e. top, bottom and left walls) are insulated. A horizontal square solid cylinder of diameter d = 0.2L and thermal conductivity k_s is considered at the center of the cavity. The inflow opening located on the left vertical adiabatic wall and the outflow opening on the opposite vertical heated wall is arranged as shown in the schematic figures and may vary in location either top or bottom position. The cavity presented in Figure 1(a) is subjected to an external flow, which enters via the bottom of the insulated vertical wall and leaves via the bottom of the opposite heated vertical wall. For reasons of brevity, this case will be referred to as BB configuration from now. When the horizontal cold jet enters into the cavity from the bottom of the insulated wall and leaves from the top of the other vertical one in Figure 1(b), this case will be referred as BT configuration. Similarly, Figues 1(c) and 1(d) are referred to as TB and TT configurations, respectively. For simplicity, the heights of the two openings are set equal to the one-tenth of the enclosure height. It is assumed that the incoming fluid flow through the inlet at a uniform velocity, U_i at the ambient temperature, T_i. The outgoing flow is assumed to have zero diffusion flux for all variables i.e. convective boundary conditions (CBC). All solid boundaries are assumed to be rigid no-slip walls.

Mathematical Model with Boundary Conditions

The flow is assumed to be two-dimensional, laminar and of constant fluid properties. The variation of density with temperature is calculated using the Boussinesq approximation. Also, the compressible work and the viscous dissipation term are neglected. After non-dimensionalization, the equations describing the flow are expressed as

$$\frac{\partial U}{\partial X}+\frac{\partial V}{\partial Y}=0 \tag{1}$$

$$U\frac{\partial U}{\partial X}+V\frac{\partial U}{\partial Y}=-\frac{\partial P}{\partial X}+\frac{1}{Re}\left(\frac{\partial^2 U}{\partial X^2}+\frac{\partial^2 U}{\partial Y^2}\right) \tag{2}$$

$$U\frac{\partial V}{\partial X}+V\frac{\partial V}{\partial Y}=-\frac{\partial P}{\partial Y}+\frac{1}{Re}\left(\frac{\partial^2 V}{\partial X^2}+\frac{\partial^2 V}{\partial Y^2}\right)+Ri\theta \tag{3}$$

$$U\frac{\partial \theta}{\partial X}+V\frac{\partial \theta}{\partial Y}=\frac{1}{Re\,Pr}\left(\frac{\partial^2 \theta}{\partial X^2}+\frac{\partial^2 \theta}{\partial Y^2}\right) \tag{4}$$

For solid cylinder, the energy equation is

$$0 = \left(\frac{\partial^2 \theta_s}{\partial X^2} + \frac{\partial^2 \theta_s}{\partial Y^2} \right) \quad (5)$$

In the above equations, the dimensionless variables are defined by

$$X = \frac{x}{L},\ Y = \frac{y}{L},\ U = \frac{u}{u_i},\ V = \frac{v}{u_i},\ P = \frac{p}{\rho u_i^2},$$

$$\theta = \frac{(T - T_i)}{(T_h - T_i)},\ \theta_s = \frac{(T_s - T_i)}{(T_h - T_i)}$$

where X and Y are the coordinates varying along horizontal and vertical directions, respectively, U and V are the velocity components in the X and Y directions, respectively, θ is the dimensionless temperature and P is the dimensionless pressure. The governing parameters, namely; the Reynolds number Re, Richardson number Ri, Prandtl numbers Pr and solid fluid thermal conductivity ratio K, are defined in the following forms

$$Re = u_i L/\nu, Ri = Gr/Re^2, Pr = \upsilon/\alpha, \text{and } K = k_s/k$$

The dimensionless forms of the boundary conditions are:

At the inlet: U = 1, V = 0, θ = 0

At the outlet: Convective boundary condition (CBC), P = 0

At all solid boundaries: U = 0, V = 0

At the heated right vertical wall: θ = 1.0

At the left, top and bottom walls: $\frac{\partial \theta}{\partial N} = 0$

At the solid-fluid interface: $\left(\frac{\partial \theta}{\partial N}\right)_{fluid} = K\left(\frac{\partial \theta_s}{\partial N}\right)_{solid}$

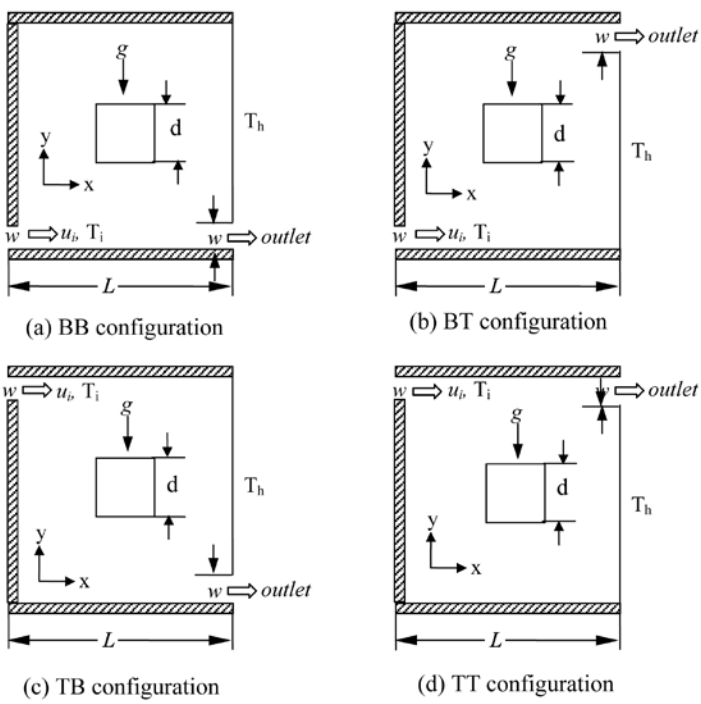

Figure 1. Schematic diagram of the physical system

where N is the non-dimensional distances either along X or Y direction acting normal to the surface.

The average Nusselt number Nu is defined as

$$Nu = \frac{hL}{k} = \frac{1}{L_h} \int_0^{L_h/L} \frac{\partial \theta}{\partial X} dY$$

and the bulk average temperature is defined as $\theta_{av} = \int \theta_d \overline{V} / \overline{V}$, where $\overline{V}$ is the cavity volume.

Numerical Procedure

The numerical procedure used in this work is based on the Galerkin weighted residual method of finite element formulation. The application of this technique is well described by (Taylor and Hood, 1973) and (Reddy, 1993). In this method, the solution domain is discretized into finite element meshes, which are composed of triangular elements. Then, the nonlinear governing partial differential equations i.e., mass, momentum and energy equations are transferred into a system of integral equations by applying Galerkin weighted residual method. Using Gauss quadrature method performs the integration involved in each term of these equations. The nonlinear algebraic equations obtained are modified by imposition of boundary conditions. These modified nonlinear equations are transferred into linear algebraic equations by using Newton's method. Finally, using Triangular Factorization method solves these linear equations.

Grid Sensitivity Check

Five different non-uniform grid systems with the following number of elements within the square cavity: 3976, 4798, 6158, 6278, and 7724 are examined. Average Nusselt number

Table 1. Comparison for grid dimensions at Re = 100, Ri = 1.0, and Pr = 0.71

Elements	3976	4798	6158	6278	7724
Nu	4.846303	4.847789	4.848895	4.852818	4.848907
θ_{av}	0.190497	0.190511	0.190514	0.190521	0.190525
Time (s)	385.219	493.235	682.985	698.703	927.359

Table 2. Comparison of nusselt number values with numerical data for Pr = 0.71

Ra	K	Nu		
		Present work	House *et al.* (1990)	Error (%)
0	0.2	0.7071	0.7063	0.11
0	1.0	1.0000	1.0000	0.00
0	5.0	1.4142	1.4125	0.12
10^5	0.2	4.6237	4.6239	0.00
10^5	1.0	4.5037	4.5061	0.00
10^5	5.0	4.3190	4.3249	0.14

at the heated surface, average temperature of the fluid in the cavity and the solution time are monitored at Re =100, Ri = 1.0 and Pr = 0.71 as shown in Table 1. The magnitude of average Nusselt number and average temperature for 6278 elements shows a very little difference with the results obtained for the other elements. For the rest of the calculation in this study, we choose a grid with 6278 elements for better accuracy.

Code Validation

In order to verify the accuracy of the numerical results and the validity of the mathematical model obtained throughout the present study, comparisons with the previously published results are necessary. But due to the lack of availability of experimental data on the particular problems along with its associated boundary conditions investigated in this study, validation of the predictions could not be done against experiment. The present numerical model is verified against one documented numerical study, namely; the numerical solutions reported by House *et al*. (1990), which is based on finite volume scheme. However, we recall here some results obtained by our model in comparison with those reported in House *et al*. (1990) for Ra = 0.0, 10^5 and three values of K = 0.2, 1.0 and 5.0. The physical problem studied by House *et al*. (1990) was a vertical square enclosure with sides of length L. The vertical walls were isothermal and differentially heated, whereas the bottom and top walls were adiabatic. A square heat conducting body with sides of length equal to L/2 was placed at the center of the enclosure. We have compared results for the average Nusselt number (at the hot wall) as shown in Table 2. The present results have an excellent agreement with the results obtained by House *et al*. (1990).

Results and Discussion

As stated earlier, the overall objective of the current investigation is to explore steady laminar mixed convection heat transfer in a vented cavity containing a solid square cylinder. The implication of varying the Reynolds numbers, Prandtl numbers and the location of inlet and outlet ports at the three values of Richardson number were emphasized. In the present research work, the solid fluid thermal conductivity ratio K = 5.0 was chosen. Physically, this value of K represents the ratio of a solid body wood and gas with properties similar to those of air. The Reynolds number Re is varied from 50 to 200, the prandtl number Pr is varied from 0.71 to 7.1 and the Richardson number varied from 0.0 to 5.0. Flow and temperature fields are presented in terms of streamline and isotherm contours, respectively. In addition, heat transfer performances were examined in terms of average Nusselt number (Nu) at the hot surface, average temperature of the fluid in the cavity and the temperature at the cylinder center in the cavity.

First, the effect of various cavity configurations on streamlines and isotherms were studied while the values of Re and Pr were fixed at 100 and 0.71, and the values of Ri was considered from 0.0 to 5.0, as shown in the Figures 2 and 3 respectively. Now at Ri = 0.0 and for the BB configuration, the induced flow enters into cavity through small inlet area and sudden expansion of the bulk fluid in the cavity occurred due to pressure rise into the cavity. Thus, the bulk fluid occupies most part of the cavity and a small recirculation cell appears just at the top of the inlet port near the left wall. Next, for Ri = 1.0, it is seen that recirculation cell spreads significantly and thereby squeezes the induced flow path. As Ri increases further to 5.0, the recirculating cell further increases in size and leads to a large change in the streamlines structure, indicating a sign of supremacy of natural convection in the upper part of the cavity. Further, when the horizontal cold jet enters into the cavity from the bottom of the insulated wall and leaves from the top of the other vertical one (i.e. for BT configuration), the recirculation cell become shrink in size and occupies the space just at the top of the inlet port adjacent to the left wall at Ri = 0.0. In this folder, as Ri increases to 1.0, the

recirculation cell becomes large and becomes into two cellular cells. Furthermore, as Ri increases to 5.0, the two cellular cells merge into a large uni-cellular, due to the supremacy of the convective current in the cavity. Next, for TB configuration, the bulk induced fluid flows throughout the cavity and a small rotating cell is developed just below the inlet port at low Ri. Further at Ri = 1.0, the existence of two cells indicates that natural convection effect is comparable with forced convection effect. Finally, at Ri = 5.0, the two cells merge into a large one, this scenario indicates that the forced convection is overwhelmed by the natural convective current. Lastly, for TT configuration, the induced flow enters into cavity through small inlet area and sudden expansion of the bulk fluid in the cavity occurred due to pressure rise into the cavity. Thus, the bulk fluid occupies most part of the cavity and a small recirculation cell appears just below the inlet port near the left wall at Ri = 0.0. Next, at Ri = 1.0, it is seen that recirculation cell becomes small in size. As Ri increases further to 5.0, the recirculating cell becomes large and shifts at the upper mid section in the cavity. Thereby, it squeezes the entrance stream to flow in it, indicating the dominant natural convection contribution in the mixed convection. Secondly, for BB configuration, it is seen from Figure 3 that the thermally influenced region is bulky in the upper part of the cavity for all values of Ri. This is because in this case the fresh fluid

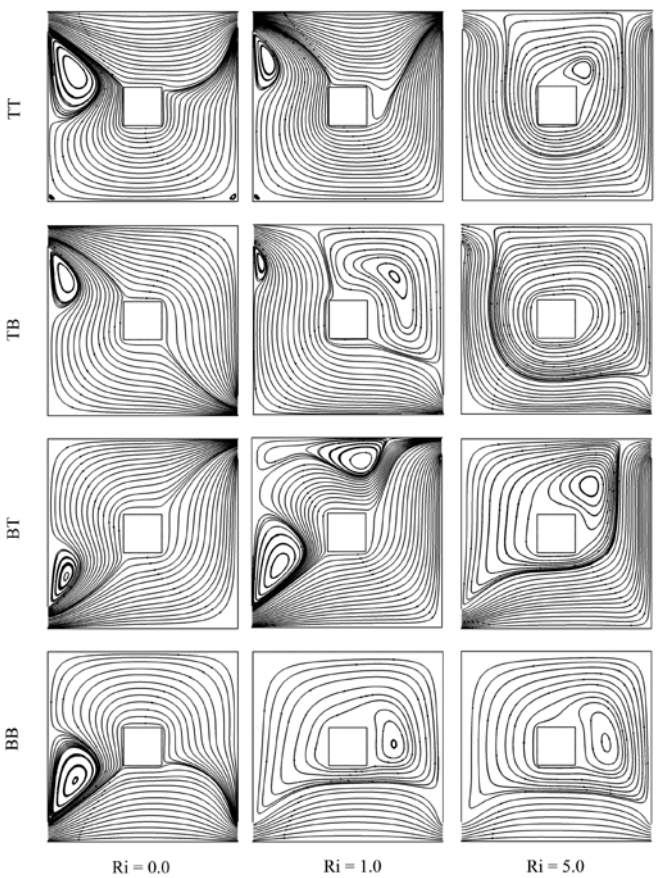

Figure 2. Streamlines for different cavity configurations and Richardson numbers while Re = 100 and Pr = 0.71

enters at the lower part of the cavity and travels the shortest distance possible leaving at the lower part in the cavity. As a result, the cold fluid cannot intimate with the hotter fluid. However, the inverse isotherm patterns are found for TT configuration at low Ri, which is because the entering fresh fluid travel the shortest distance possible leaving, but it come into intimate mixing with the hotter fluids before leaving the cavity. Next, at Ri = 1.0 and for TT configuration the isotherms become clustered near the heat source, indicating conduction and forced convection dominated heat transfer in the cavity. Furthermore, as Ri increases to 5.0, the concentrated thin thermal layer is seen near the heated wall and nonlinearity of the isotherms is found. Moreover, the isotherms are clustered near the heat source for the BT and TB configurations at low Ri, which points to the forced convection and conduction-like heat transfer at the vicinity of the heat source. This is because the fresh fluid entering the cavity travels the long possible distance before leaving the cavity and come into intimate mixing with the hotter fluids. As Ri increases to 1.0, nonlinearity in the isotherms found for these cases. Furthermore, as Ri increases to 5.0, nonlinearity of the isotherms becomes higher and plume formation is philosophical for these cases, indicating

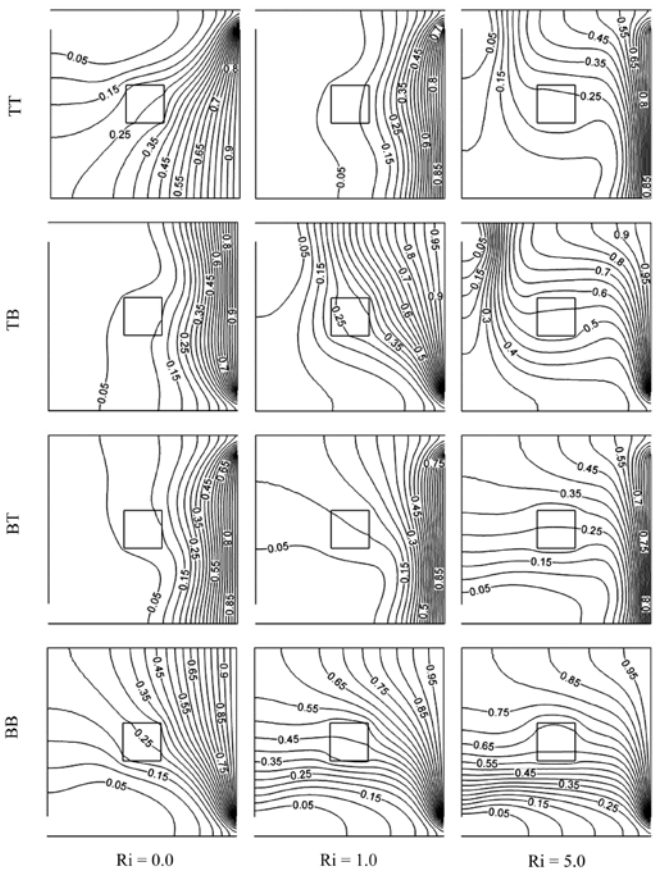

Figure 3. Isotherms for different cavity configurations and Richardson numbers while Re = 100 and Pr = 0.71

well established natural convection heat transfer in the cavity.

The effect of Richardson number on the average Nusselt number at the hot surface, average temperature of the fluid in the cavity and the temperature at the cylinder center in the cavity for different cavity configurations are shown in Figure 4. As Ri increases, the average Nusselt number at the heated surface gradually increases for the BT and TT configurations, while the values of Nu sharply decreases in the forced convection dominated region and sharply increases in the natural convection dominated region for the TB configuration. But the values of Nu were independent of the values of Ri for the BB configuration. Maximum average Nusselt number was obtained, without the effect of Ri for the BT configuration. This is because the induced cold fluid flows over the heated surface. Thus, heat transfer was enhanced by forced convection rather than natural convection. On the other hand, the average temperature of the fluid in the cavity and the temperature at the cylinder center in the cavity were not monotonic with the increase of Ri for a particular cavity configuration. For a fixed value of Ri, the values of θ_{av} and θ_c are the lowest for BT configuration at Ri θ 0.8, but beyond these values of Ri, the values of ≤ and θ_c are the lowest for TT configuration.

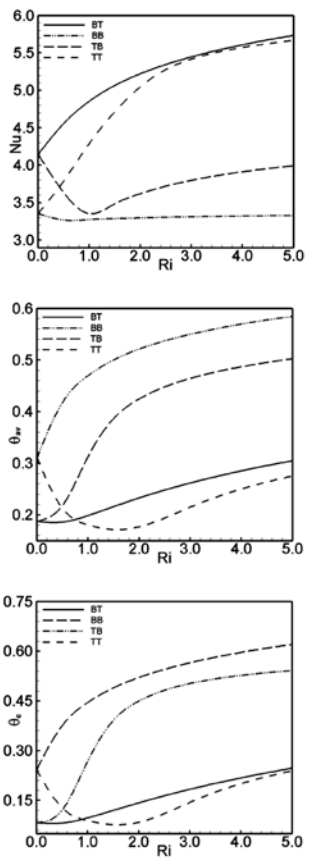

Figure 4. Effect of Richardson number on (a) average Nusselt number, (b) average temperature and (c) temperature at the cylinder center for various cavity configurations, while Re = 100 and Pr = 0.71

The effect of Reynolds numbers *Re* on the fluid flow and temperature distribution for different convective regimes in the cavity are illustrated in the Figures 5 and 6 by plotting the streamlines and isotherms for Re = 50, 100, 150 and 200 and various Ri (= 0.0, 1.0 and 5.0). The basic flow structure in the absence of natural convection effect is presented in the left bottom corner of Figure 5 at Re = 50. From this figure, it is clear that the open lines become bifurcate near the cylinder and occupy the totality of the cavity space. The corresponding isotherms result from combined effects of conduction and forced convection is shown in the left bottom corner of Figure 6, which indicated that a large area of the cavity remains at higher temperature. For Re = 100 and Ri = 0.0, it can be seen from the Figure 5 that a small recirculating cell was developed just at the top of the inlet port and the recirculating cell became large with the increased of Re (= 150 and 200). Moreover, the corresponding isotherm becomes more tightened at the vicinity of the heated wall with increasing Re as shown in the Figure 6. On the other hand, at any particular Reynolds number, there is a marked changed in flow patterns and isotherms as the flow regime changes from dominant forced convection to dominant natural convection with increasing Ri.

Figure 7(a) shows a very illustrative picture of how the heat was transferred in accordance with Re and Ri. Keeping Re constant, the average Nusselt number Nu at the heated surface increases gradually with increasing values of Ri. Also, the average Nusselt number at the heated surface increases as Re increases with fixed Ri. Therefore, it can be concluded that more heat transfer from the heat source is expected in the case of large parameter value of Re or Ri. It is also of interest to examine the average temperature of the fluid and the temperature at the cylinder center in the cavity for various Re and Ri, which are shown in Figure 7 (b-c). The average temperature of the fluid and the temperature at the cylinder center in the cavity increases with Ri for the different values of Re considered. On the other hand, for a fixed value of Ri, the values of θ_{av} and θ_c are the lowest for the largest Re.

Lastly, the effect of Prandtl numbers on the flow and thermal field are presented in Figures 8-9. For low Ri and Pr, it is seen that the through stream occupies most of the part of the cavity and a small vortex of low speed appears immediately at the top of the inlet port of the cavity. Making a comparison of the streamlines at Ri = 0.0 for various Pr, no significant difference is found. On the other hand, when Ri increases, the small vortex sharply increases for the lower values of Pr (= 0.71, 1.0, and 3.0), but gradually increases

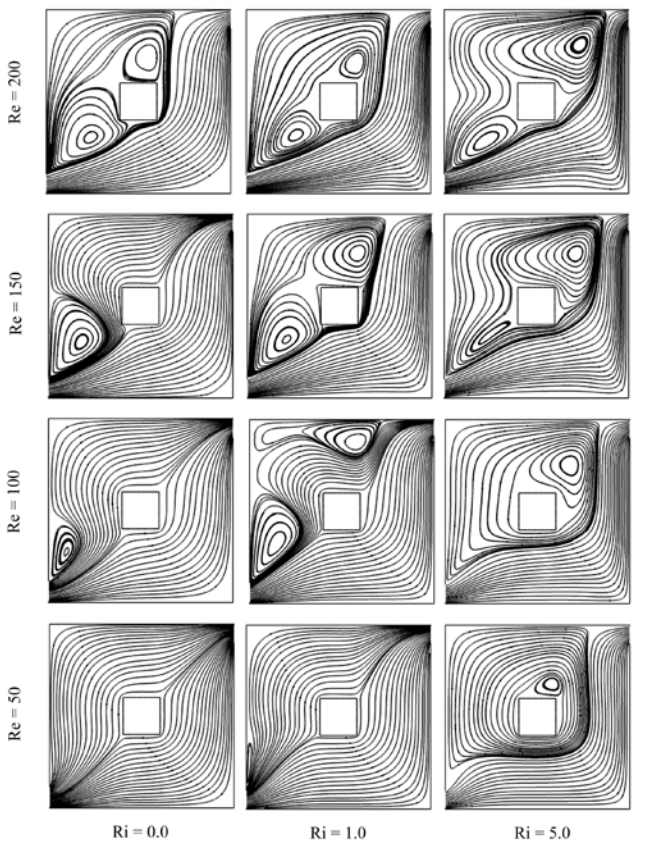

Figure 5. Streamlines for BT configuration at various Reynolds number and Richardson number, while Pr = 0.71

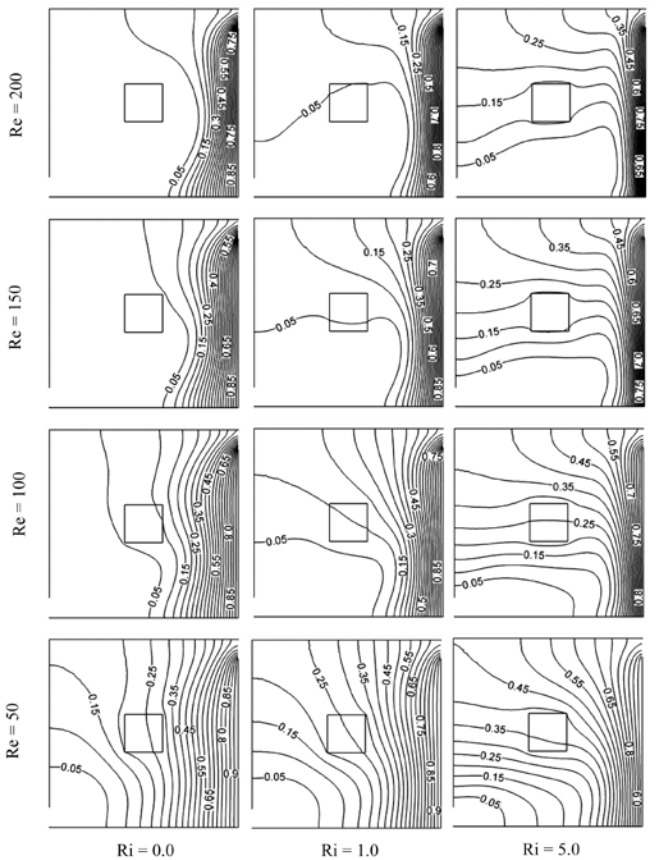

Figure 6. Isotherms for BT configuration at various Reynolds number and Richardson number, while Pr = 0.71

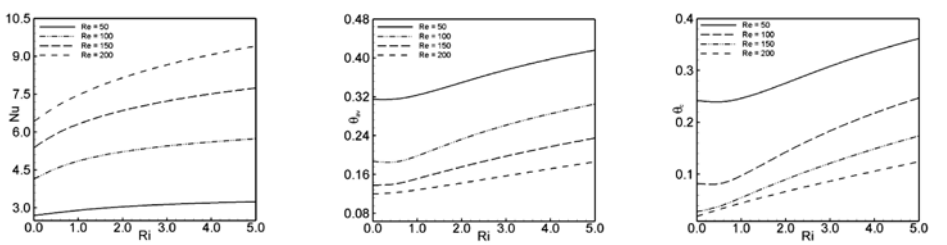

Figure 7. Effect of Richardson number on (a) average Nusselt number, (b) average temperature and (c) temperature at the cylinder center for BT configuration at various Reynolds number, while Pr = 0.71

for the highest Pr. These isotherms are almost linear and parallel to the heated surface in the cavity for the lower Pr (= 0.71 and 1.0) and Ri = 0.0. This points out to the diffusive heat transfer in the cavity. As Ri increases, nonlinearity in isotherms are seen and plume formation initiate in the case of the lower values of Pr (= 0.71 and 1.0), which indicates the supremacy of natural convection heat transfer over forced convection and conduction in the cavity. On the other hand, with the increase of the values of Pr (= 3.0, 7.1) the isotherms become bunch near the heated surface due toconductive heat transfer at the vicinity of the hot wall in the cavity, and the thermal boundary layer near the hot wall is thinner for higher Pr than that of the lower Pr for the different values of Ri.

The effects of varying Ri on average Nusselt number variation along the hot wall, average temperature of the fluid and the temperature at the cylinder center in the cavity for different values of Pr are illustrated in Figure 10. In general, due to higher temperature gradients associated with higher values of Pr, the level of Nu increases with Pr increases for different values of Ri. On the other hand, for a particular value of Pr, the value of Nu increases sharply with Ri. Furthermore, it is seen that the average temperature of the fluid in the cavity increases gradually with Ri for the lower values of Pr (= 0.71 and 1.0), but

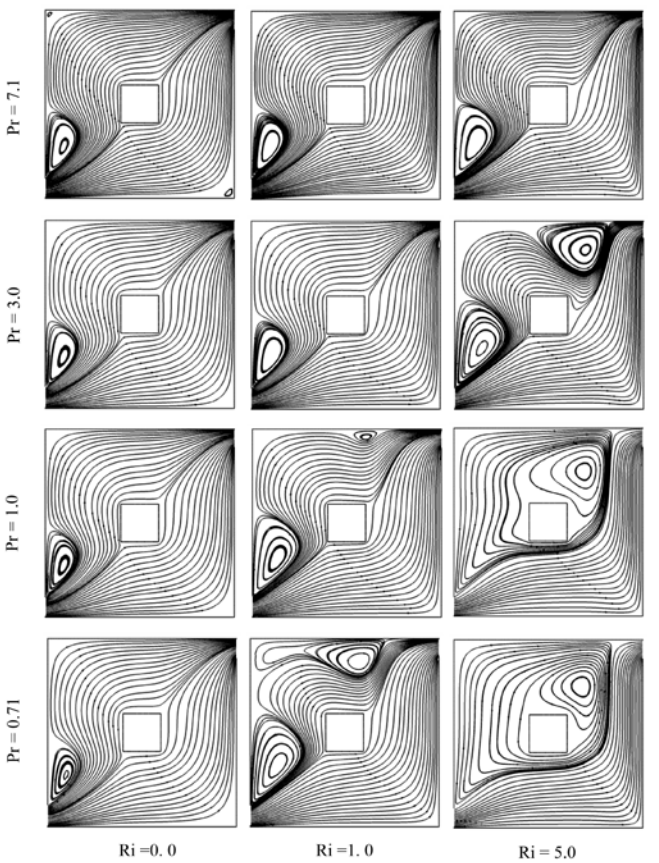

Figure 8. Streamlines for BT configuration at different values of Prandtl number and Richardson number, while Re = 100

decreases gradually with Ri for the higher values of Pr (= 3.0 and 7.1). The temperature at the cylinder center increases gradually with Ri for the lower values of Pr (= 0.71 and 1.0), but become independent of Ri for the higher values of Pr (= 3.0 and 7.1). On the other hand, the average fluid temperature and temperature at the cylinder center are found lowest for the largest value of Pr.

Conclusions

The flow and heat transfer are studied in a vented square cavity with a centered heat conducting horizontal square cylinder of diameter D = 0.2. The effect of Reynolds number Re, Prandtl number Pr and cavity configurations at the three convective regimes on the flow pattern and heat transfer area are examined for laminar ranges of Re and Pr. The following are some of the important observations made:

- Cavity orientation has a great influence on the streamlines and isotherms distributions at the three convective regimes. The average Nusselt numbers at the hot wall have been used to compare the heat transfer rate among different configurations. Results show that the configuration BT has the highest heat transfer rate, whereas the configuration BB has the less effective heat transfer rate at the three convective regimes. Moreover, bulk average temperature and cylinder center temperature

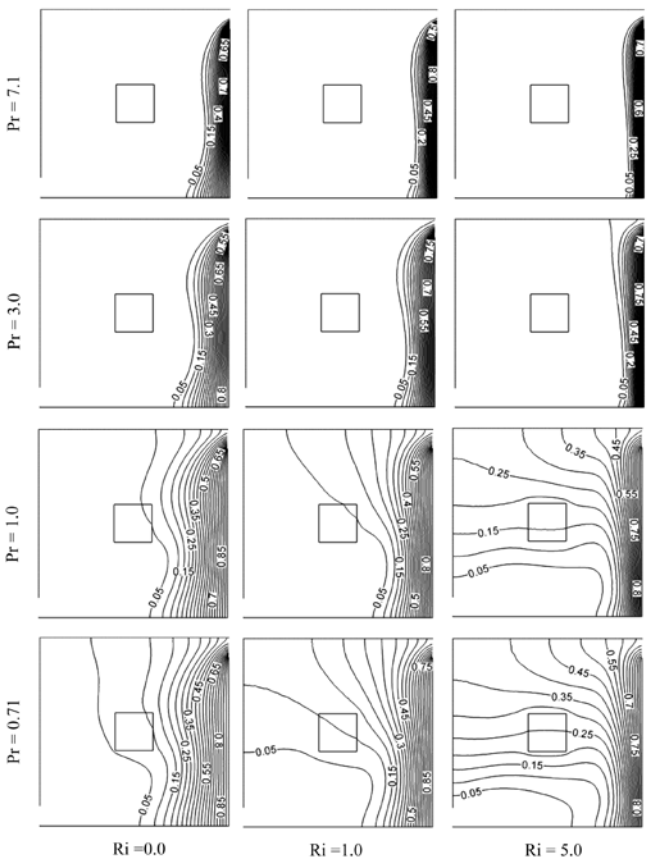

Figure 9. Isotherms for BT configuration at different values of Prandtl number and Richardson number, while Re = 100

are the lowest for BT configuration in the forced convection dominated region and for TT configuration in the free convection dominated region.

- Forced convection parameter, Reynolds number (Re) has a significant effect on the streamlines in the pure forced and mixed convection region, but has significant effect on isotherms in the three convective regimes. The average Nusselt numbers at the heated surface is always upper and the average fluid temperature as well as cylinder center temperature in the cavity are inferior for the largest value of Re.
- Prandtl number (Pr) has a significant effect on the streamlines in the pure mixed convection and free convection dominated region, but has significant effect on isotherms in the three convective regimes. Maximum average Nusselt number, minimum average fluid temperature and cylinder center temperature are found for the highest Pr = 7.1.

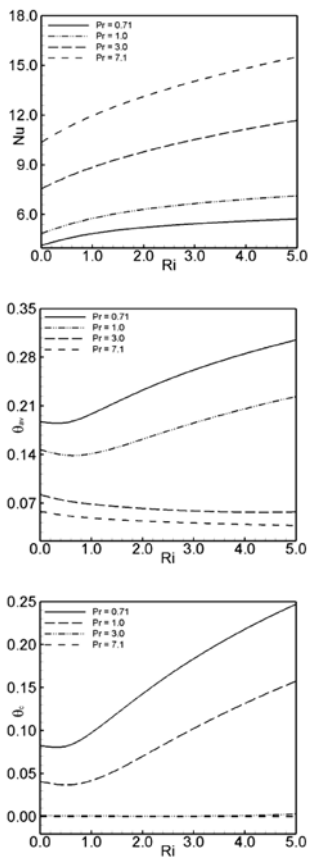

Figure 10. Effect of Richardson number on (a) average Nusselt number, (b) average temperature and (c) temperature at the cylinder center for BT configuration at various values of Prandtl number, while Re = 100

Acknowledgements

The authors like to express their gratitude to the Department of Mathematics, Bangladesh University of Engineering and Technology, for providing computer facility during this work.

Nomenclature

d	dimensional diameter of the cylinder
D	dimensionless diameter of the cylinder
g	gravitational acceleration
h	convective heat transfer coefficient
k	thermal conductivity of fluid
k_s	thermal conductivity of the cylinder
K	Solid fluid thermal conductivity ratio
L	length of the cavity
Nu	average Nusselt number
p	dimensional pressure
P	dimensionless pressure
Pr	Prandtl number
Ra	Rayleigh number
Re	Reynolds number
Ri	Richardson number
T	dimensional temperature
u, v	dimensional velocity components
U, V	dimensionless velocity components
$\overline{V}$	cavity volume
ω	height of the opening
x, y	Cartesian coordinates
X, Y	dimensionless Cartesian coordinates

Greek symbols

α	thermal diffusivity
β	thermal expansion coefficient

v	kinematic viscosity
θ	dimensionless temperature
ρ	density of the fluid

Subscripts

av	average
h	heated wall
i	inlet state
c	cylinder center
s	solid

References

Hsu, T.H. and Wang, S.G. (2000). Mixed convection in a rectangular enclosure with discrete heat sources, Numer. Heat Transfer. Part A, 38:627-652.

Angirasa, D. (2000). Mixed convection in a vented enclosure with isothermal vertical surface. Fluid Dyn. Res., 26:219-233.

Omri, A. and Nasrallah, S.B. (1999). Control volume finite element numerical simulation of mixed convection in an air-cooled cavity, Numerical Heat Transfer, Part A, 36:615-637.

Singh, S. and Sharif, M.A.R. (2003). Mixed Convection cooling of a rectangular cavity with inlet and exit openings on differentially heated side walls. Numerical Heat Transfer, Part A, 44:233-253.

Manca, O., Nardini, S., Khanafer, K., and Vafai, K. (2003). Effect of heated wall position on mixed convection in a channel with an open cavity. Experimental Heat Transfer, 43:259-282.

Manca, O., Nardini, S., and Vafai, K. (2006). Experimental investigation of mixed convection in a channel with an open cavity. Numerical Heat Transfer, Part A, 19:53-68.

Papanicolaou, E. and Jaluria, Y. (1990). Mixed convection from an isolated heat source in a rectangular enclosure. Numerical Heat Transfer, Part A, 18:427-461.

Papanicolaou, E. and Jaluria, Y. (1993). Mixed convection from a localized heat source in a cavity with conducting walls: A numerical study. Numerical Heat Transfer, Part A, 23:463-484.

House, J.M., Beckermann, C., and Smith, T.F. (1990). Effect of a centered conducting body on natural convection heat transfer in an enclosure. Numerical Heat Transfer, Part A, 18:213-225.

Lacroix, M. and Joyeux, A. (1995). Natural convection heat transfer around heated cylinder inside a cavity with conducting walls. Numer. Heat Transfer, Part A, 27:335-349.

Braga, E.J. and de Lemos, M.J.S. (2005). Laminar natural convection in cavities filed with circular and square rods. Int. Commun. in Heat and Mass Transfer, 32:1289-1297.

Lee, J.R. and Ha, M.Y. (2005). A numerical study of natural convection in a horizontal enclosure with a conducting body. Int. J. of Heat and Mass Transfer, 48:3308-3318.

Taylor, C. and Hood, P. (1973). A numerical solution of the Navier-Stokes equations using finite element technique. Computer and Fluids 1, 1:73-89.

Reddy, J.N. (1993). An introduction to the finite element method. McGraw-Hill, New York.

Rahman, M.M., Alim, M.A., and Mamun, M.A.H. (2009). Finite element analysis of mixed convection in a rectangular cavity with a heat-conducting horizontal circular cylinder. Nonlinear Analysis: Modelling and Control, 14 (2):217-247.